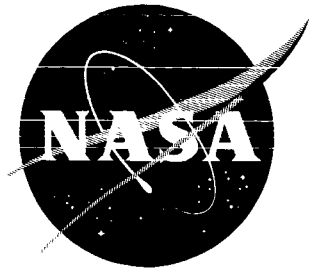

TECHNICAL MEMORANDUM

X-487

DESIGN AND PERFORMANCE OF A SIX-STAGE 8-INCH-MEAN-DIAMETER REENTRY TURBINE

By David G. Evans, William D. Guthrie,
and Charles A. Wasserbauer

Lewis Research Center
Cleveland, Ohio

NATIONAL AERONAUTICS AND SPACE ADMINISTRATION

WASHINGTON

August 1962

NATIONAL AERONAUTICS AND SPACE ADMINISTRATION

TECHNICAL MEMORANDUM X-487

DESIGN AND PERFORMANCE OF A SIX-STAGE 8-INCH-MEAN-DIAMETER REENTRY TURBINE*

By David G. Evans, William D. Guthrie, and Charles A. Wasserbauer

SUMMARY

The performance characteristics of a turbine designed to operate at a high pressure ratio with a low specific fuel consumption were investigated. The turbine was a six-stage, 8-inch-mean-diameter reentry turbine designed for a nominal total- to static-pressure ratio of 210, an overall blade- to jet-speed ratio of 0.161, and a first-stage throat area of 0.0135 square inch. The turbine was similar in design configuration and weight flow to a four-stage, 4-inch-mean-diameter reentry turbine investigated previously.

At design speed and pressure ratio, the equivalent-air specific work output was 46 Btu per pound at a static efficiency of 0.47. Interstage pressure measurements indicated that the first- and second-stage pressure ratios were greater than the design specification, possibly because of flow leakage upstream of the second- and third-stage stators. At all but the lowest pressure ratios investigated, the static-pressure distribution, which remained unchanged throughout the turbine, indicated that the last-stage stator was operating choked as specified in the design.

INTRODUCTION

Total weight is an important factor to be considered in selecting and designing the turbodrive unit for an auxiliary power system. In order to minimize the weight of the system, the turbine must be able to convert a maximum of its available fuel energy into useful work. The turbine must therefore be of a high-specific-work low-weight-flow design.

*Title, Unclassified.

Achieving the maximum possible power output from each pound of fuel expended requires a high turbine-inlet enthalpy, a high overall pressure ratio, and a high overall efficiency. Multistage turbines must therefore be considered in order to obtain reasonable overall efficiencies at high overall pressure ratios with the assumption that turbine speeds are limited either by blade stress limitations or by the particular system requirements.

Several types of conventional and unconventional high-specific-work low-weight-flow turbines are potentially suitable for this application. Multistage reentry type turbines have been considered at the Lewis Research Center because many of their unique features appear appropriate.

In the reentry turbine, "multistaging" is accomplished by passing the flow through a single rotor several times. Reentry ducts direct the flow between successive stages located in segments around the rotor annulus. The last stages act to cool the rotor and permit higher turbine-inlet temperatures and, therefore, higher turbine-inlet enthalpies, generally, than would be possible for conventional turbines.

The design and performance characteristics of two such reentry turbines are given in references 1 and 2. They are a 11.53-inch-mean-diameter three-stage and a 4.0-inch-mean-diameter four-stage reentry turbine designed for total- to static-pressure ratios of 10.1 and 55.66 and blade- to jet-speed ratios of 0.220 and 0.194, respectively. Several additional reentry turbine configurations have been investigated, such as a two-stage impulse reentry turbine designed for a pressure ratio of 11.76 and a blade- to jet-speed ratio of 0.129 (ref. 3).

Although the performance characteristics demonstrated by these turbines approached the requirements desired for auxiliary power systems, it was felt that the performance capability of the reentry turbine could be extended by utilizing higher pressure ratios and increasing the number of stages. In order to verify this supposition, a six-stage reentry turbine having a nominal total- to static-pressure ratio of 210 was designed and experimentally investigated. Even though the performance of the four-stage reentry turbine (ref. 2) was not available for evaluation at the time of design, the six-stage reentry turbine was designed in approximately the same manner, as noted later in the Blade Design and the Reentry Duct Design sections, and for approximately the same weight flow. The reentry system was of the type that diffused the flow at the exit of each stage to a relatively low velocity, directed it over the rotor, then reaccelerated and turned it through a conventional stator section to the next stage. The rotor mean diameter and blade height were double those of the four-stage reentry turbine to provide for the additional annulus area required for the two additional stages. The results of interstage as well as overall performance measurements made during the experimental phase of the investigation are presented herein.

SYMBOLS

g	gravitational constant, 32.17 ft/sec^2
Δh	specific work output, Btu/lb
J	mechanical equivalent of heat, 778.16 ft-lb/Btu
N	rotational speed, rpm
P_r	turbine inlet-total- to exit-static-pressure ratio, p'_0/p_6
p	absolute pressure, lb/sq ft
U	blade velocity, ft/sec
V	absolute gas velocity, ft/sec
V_j	ideal jet speed corresponding to total- to static-pressure ratio across turbine, $\sqrt{2gJ\ \Delta h_{id}}$
W	relative gas velocity, ft/sec
w	weight-flow rate, lb/sec
γ	ratio of specific heats
δ	ratio of turbine-inlet total pressure to NACA standard sea-level pressure, $p'_0/2116$
ϵ	function of γ, used to correct weight flow to inlet conditions at NACA standard sea-level atmosphere, $\epsilon = \frac{0.740}{\gamma}\left(\frac{\gamma+1}{2}\right)^{\gamma/(\gamma-1)}$
η	static efficiency, based on total- to static-pressure ratio across turbine
θ_{cr}	squared ratio of turbine-inlet flow critical velocity to that of NACA standard sea-level atmosphere, $(V_{cr,0}/1019)^2$
λ	speed-work parameter, $U_m^2/gJ\ \Delta h$
ν	blade- to jet-speed ratio, U_m/V_j
τ	torque, in.-lb

Subscripts:

cr	conditions corresponding to Mach number of 1
id	ideal
in	stage inlet
m	mean-radius value
out	stage exit
s	stage
u	tangential component
x	axial component
0	turbine inlet (see fig. 4)
1	first reentry duct
2	second reentry duct
3	third reentry duct
4	fourth reentry duct
5	fifth reentry duct
6	turbine exit

Superscript:

'	absolute total state

TURBINE DESIGN

The turbine was designed for the following requirements, which were based on NACA equivalent-air conditions at the turbine inlet (turbine-inlet temperature of 518.7° R and pressure of 2116 lb/sq ft abs):

Equivalent weight flow, $w\sqrt{\theta}\ \epsilon/\delta$, lb/sec 0.00447
Equivalent blade velocity, $U_m/\sqrt{\theta_{cr}}$, ft/sec 356.0
Nominal overall total- to static-pressure ratio, P_r 210
Number of turbine stages 6

These requirements resulted in the following design values:

Blade- to jet-speed ratio, ν 0.161
Mean wheel diameter, in. 8.0
Blade height, in. 0.25
Equivalent rotational speed, $N/\sqrt{\theta_{cr}}$, rpm 10,200
Total arc of admission, deg 318.8

Stage Characteristics

The following stage requirements were incorporated in the design:

	Stage					
	1	2	3	4	5	6
Speed-work parameter, λ_s	0.2	0.5	0.5	0.5	0.5	0.5
Static efficiency, η_s	0.54	0.70	0.70	0.70	0.70	0.70
Resulting nominal stage total- to static-pressure ratio, p'/p_s	5.2	1.7	1.9	2.0	2.3	2.7

Additional requirements were

(1) Constant hub and tip radii across the rotor and stator sections

(2) Zero absolute whirl leaving stages 2 to 6

(3) Stator discharge free-stream flow angle of 15° from the plane of the rotor, stages 2 to 6

Stage velocity diagrams and area ratios were then computed from these requirements in addition to the following assumptions:

(1) 100 Percent of the weight flow entered each stage.

(2) The velocity head at the exit of each stage was lost in diffusion.

(3) Stator losses were equal to 5 percent of the stage inlet pressure.

The design velocity diagrams satisfying the preceding requirements and assumptions are shown in figure 1. The design resulted in equal relative whirl components entering and leaving the rotor ($W_{u,in} = W_{u,out}$). The velocities shown are for equivalent-air conditions at the turbine inlet. The first-stage stator and rotor, and to a lesser degree the last-stage stator, were supersonic; the remaining stages were subsonic. The absolute stator-discharge velocity ratios ($(V/V_{cr})_{in}$, fig. 1) for stages 1 to 6, respectively, were 1.311, 0.808, 0.853, 0.905, 0.970, and 1.051. The rotor-inlet relative velocity ratios $(W/W_{cr})_{in}$ for stages 1 to 6, respectively, were 1.061, 0.461, 0.490, 0.523, 0.565, and 0.619.

Blade Design

The first-stage stator was designed in essentially the same manner as the four-stage reentry turbine (ref. 2). It was designed to turn and to accelerate the flow to sonic velocity in a single smoothly convergent channel with a rectangular cross section, and then to expand it supersonically to a critical velocity ratio V/V_{cr} of 1.311 in a minimum-length sharp-cornered supersonic section downstream of the stator throat. A loss in total pressure of 3 percent was assumed upstream of the throat and 2 percent downstream of the throat, which, for the design weight flow, resulted in a first-stage throat area of 0.0135 square inch. The method used to obtain the shape of the divergent supersonic section is described in reference 4. The resulting dimensions, mean-radius channel profile, and channel coordinates of the stator are given in figure 2.

The stators for the remaining five stages were designed to turn and to accelerate the flow in smoothly convergent channel passages with rectangular cross sections. Each stage was identical for simplicity of fabrication (fig. 2). In order to achieve the design supersonic exit velocity for the sixth-stage stator, expansion downstream of the throat was assumed.

The rotor was not an impulse type such as the one used in the four-stage reentry turbine but was designed to provide for a small amount of

reaction as well as zero suction surface diffusion at the mean-radius blade section for stages 2 to 6. Continuity across the rotor and equilibrium in the radial-axial plane and across the blade channel from the suction surface to the pressure surface was satisfied. In general, the design procedure corresponded to that of reference 1 except that a single mean-section blade design, rather than a three-section blade design, was used with a resulting constant nontwisted blade section from hub to tip. The mean-radius blade dimensions, profile, and coordinates are shown in figure 2. Running clearances are also shown in figure 2. In addition, the design blade-surface and midchannel velocity distributions are shown for the sixth stage in figure 3. The distribution, which is similar for stages 2 to 6, indicates almost no deceleration (diffusion) of flow along the suction surface.

Since the rotor channel was designed to satisfy the subsonic requirements of stages 2 to 6, the design was not compatible with the first-stage supersonic area-ratio requirements. Because the first stage was operating over a small arc of admission compared with the remaining stages, it was felt that the spreading effects of the jet leaving the stator would tend to correct for the mismatch.

Reentry Duct Design

The reentry passages were designed in essentially the same manner as the four-stage reentry turbine (ref. 2). The six-stage reentry configuration is shown schematically in figure 4. The ducts were designed to diffuse the flow leaving the rotor to a low velocity, to direct it, and then to reaccelerate it into the segment of the stator annulus corresponding to the next stage. The diffusion and reacceleration were accomplished by varying the hub radius linearly along the sections entering and leaving the ducts from an opening of 0.250 inch at the blade end to an opening of approximately 0.875 inch, which gave an area ratio of approximately 4. From the diffuser, the flow was turned 180° and was further diffused by an area change of approximately 1.3. The duct inlets were placed relative to the preceding stator section in the same manner as in the four-stage reentry turbine.

APPARATUS, INSTRUMENTATION, AND PROCEDURE

Photographs of the turbine and of the test facility used for the investigation are shown in figures 5 and 6. The turbine rotor blades and disk were machined integrally from a forging of high-temperature stainless steel. The stator blades and the stator hub ring were also machined in the same manner; the stator tip ring was brazed in place after machining. All blade profiles were machined to within 0.001 inch of the true shape. The turbine casing including the reentry system was fabricated of stainless steel and brazed together.

The turbine was operated on pressurized air at nominal inlet conditions of 240° F and 115 pounds per square inch gage. Weight flow was measured with a calibrated thin-plate orifice. Since the first-stage stator was choked, the equivalent weight flow did not vary over the range of speeds and pressure ratios investigated. The power output of the turbine was absorbed by a cradle-mounted airbrake and measured with a strain gage load cell calibrated before and after the performance test. Turbine speeds were measured with a magnetic pickup and a 10-tooth sprocket gear mounted on the rotor shaft in conjunction with an electronic tachometer.

Overall and interstage pressure measurements were made from static taps located on the turbine inlet and exhaust ducts and reentry ducts (fig. 4). Temperatures were measured using bare wire thermocouples located in the same areas.

The experimental performance of the turbine was obtained from data taken over a range of turbine speeds and pressure ratios. Speeds were varied from either 30 or 70 percent design speed to 100 percent design speed. Pressure ratios were varied from 131 to 238 by varying the outlet static pressure. Dewpoint measurements were made of the pressurized air prior to performance testing and were checked against interstage and exit temperature measurements to avoid operation below the dewpoint, where freezing and condensation shocks could have affected the performance.

Turbine bearing, seal, and disk windage losses were obtained by replacing the rotor with a bladeless disk of equal dimensions and then by motoring the turbine with the airbrake from 0 to 100 percent of design speed. The pressures measured in the turbine casing on either side of the turbine disk during performance testing were duplicated to simulate disk windage losses and bearing thrust loads. The resultant torque, measured with the strain gage load cell, amounted to approximately 31 percent (3.8 in.-lb) of the shaft torque output of the turbine at design speed and pressure ratio.

Turbine efficiency was computed as the ratio of the blade output (shaft output plus bearing, seal, and windage losses) to the ideal rotor-blade output. The ideal rotor blade output was obtained from National Bureau of Standards tables (ref. 5) for the measured values of turbine-inlet total temperature and pressure and -outlet static pressure. Turbine torque, specific work output, speed, and weight flow were corrected to standard NACA sea-level equivalent-air conditions.

RESULTS AND DISCUSSION

Overall Turbine Performance

Overall turbine performance is presented in figures 7 to 9 and is based on the rotor-blade output (shaft output plus bearing, seal, and

windage losses), as mentioned previously. In figure 7 the equivalent-air specific work output $\Delta h/\theta_{cr}$ and static efficiency η are shown plotted against the total- to static-pressure ratio P_r over the range of speeds investigated. At 100 percent design speed and at the nominal design total- to static-pressure ratio of 210, the equivalent specific work output was 46 Btu per pound at a static efficiency of 0.47. Rotor limiting loading was not obtained, as indicated by the gain in the equivalent specific work output up to 47 Btu per pound at the highest pressure ratio investigated, 238.

The observed choked equivalent weight flow was 0.00446 pound per second, which compared with the design value of 0.00447 pound per second and resulted in a first-stage stator flow coefficient of 0.97.

In figure 8, the static efficiency η is replotted against the blade- to jet-speed ratio ν for the design total- to static-pressure ratio. Experimental points were obtained down to 30 percent design speed. The general shape of the curve approximates those of conventional multistage turbines. Corresponding curves and design point values for the turbines of references 1 to 3 are also shown on the figure for comparison. The design-point static efficiency of the four-stage reentry turbine was 0.432, obtained at a total- to static-pressure ratio of 55.66 and a blade- to jet-speed ratio of 0.194. At an equivalent blade- to jet-speed ratio of 0.161, there was a six-point difference in efficiency between the four-stage and the six-stage reentry turbines, which indicated the improvement in overall performance of the six-stage over the four-stage turbine.

In figure 9, equivalent shaft and blade torque $\tau\epsilon/\delta$ is shown plotted against percent design speed at the nominal design total- to static-pressure ratio P_r of 210. Experimental points were obtained from 30 to 100 percent of design speed. Extrapolation of the blade torque curve to zero speed indicated that zero-speed torque was approximately 1.58 times the design speed torque. Furthermore, the variation in blade torque with speed was approximately linear, as with conventional full-admission multistage turbines. The turbine bearing, seal, and disk windage losses account for the difference between the two curves.

Interstage Characteristics

The interstage pressure measurements made during the performance investigation are presented in figure 10. The distributions obtained at the nominal design overall total- to static-pressure ratio of 210, and at 131, 175, and 238 are shown plotted at each station (see fig. 4) across the turbine. The interstage static pressures were measured in the reentry ducts and presented as ratios to the inlet total pressure. The measurements were obtained at design speed.

Fair agreement was obtained between the actual and the design static-pressure distribution; however, there was some overexpansion across the first and second stages, and underexpansion across the latter stages compared with design. The tendency to overexpand across the first stage was observed previously in the three-stage reentry turbine (ref. 1), on which more detailed interstage measurements were made. These measurements indicated that the cause was due to large flow leakage losses out of the first stage. The losses reduced the amount of flow entering the second stage, which increased the effective area ratio between the first and second stages and hence the pressure ratio of the first stage. As may be noted in figure 10, the stage static-pressure distribution remained unchanged over the range of pressure ratios investigated above 175, which indicated that the last-stage stator was operating choked as specified in the design.

SUMMARY OF RESULTS

The results of the investigation of the six-stage, 8-inch-mean-diameter reentry turbine designed for a nominal pressure ratio of 210 and a blade- to jet-speed ratio of 0.161 are summarized as follows:

1. At design speed and design pressure ratio, the equivalent-air specific work output was 46 Btu per pound at a static efficiency of 0.47.

2. Torque-speed characteristics appeared comparable with conventional full-admission multistage turbines. Zero-speed torque was approximately 1.58 times the design-speed torque at design pressure ratio.

3. Fair agreement was obtained between the design and experimental static-pressure distribution across the turbine. Some overexpansion of the flow across the first and second stages appeared to be caused by flow leakage out of the stages. The distribution remained unchanged above a pressure ratio of 175 and indicated that the last-stage stator was choked as specified.

Lewis Research Center
National Aeronautics and Space Administration
Cleveland, Ohio, February 9, 1962

REFERENCES

1. Evans, David G.: Design and Experimental Investigation of a Three-Stage Multiple-Reentry Turbine. NASA MEMO 1-16-59E, 1959.

2. Wong, Robert Y., Darmstadt, David L., and Monroe, Daniel E.: Investigation of a 4.0-Inch-Mean-Diameter Four-Stage Reentry Turbine for Auxiliary Power Drives. NASA TM X-152, 1960.

3. Wong, Robert Y.: Experimental Investigation of a 5.25-Inch-Mean-Diameter Two-Stage Reentry Turbine Suitable for High-Energy Auxiliary Drive Applications. NASA TM X-474, 1961.

4. Edelman, Gilbert M.: The Design, Development, and Testing of Two-Dimensional Sharp-Cornered Supersonic Nozzles. Rep. 22, M.I.T., May 1, 1948.

5. Hilsenrath, Joseph, et al.: Tables of Thermal Properties of Gases. Cir. 564, NBS, Nov. 1, 1955.

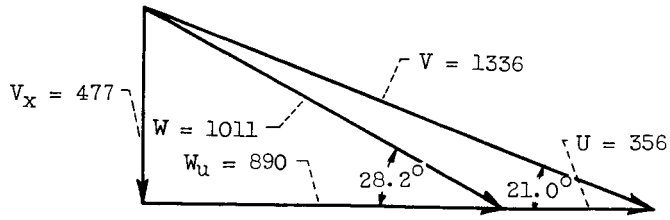

Stage 1; station between stator exit and rotor inlet

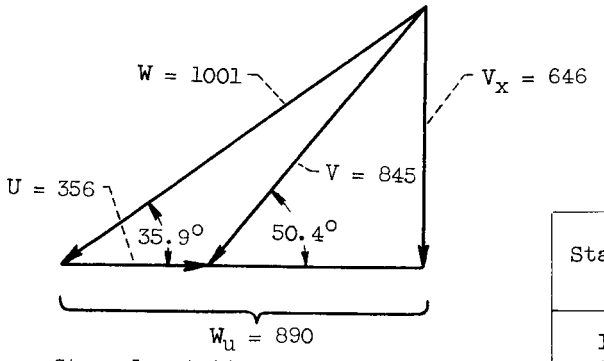

Stage 1; station at rotor exit

Stage	$\left(\frac{V}{V_{cr}}\right)_{in}$	$\left(\frac{V}{V_{cr}}\right)_{out}$	$\left(\frac{W}{W_{cr}}\right)_{in}$	$\left(\frac{W}{W_{cr}}\right)_{out}$
1	1.311	0.921	1.061	1.151
2	.808	.299	.461	.502
3	.853	.318	.490	.533
4	.905	.340	.523	.569
5	.970	.368	.565	.614
6	1.051	.404	.619	.670

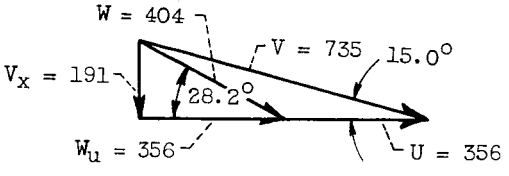

Stages 2 to 6; station between stator exit and rotor inlet

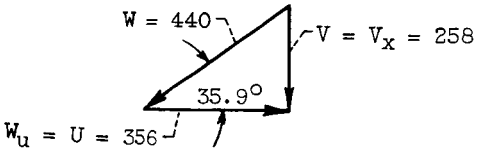

Stages 2 to 6; station at rotor exit

Figure 1. - Six-stage reentry turbine mean-diameter design velocity diagrams for equivalent-air conditions at turbine inlet.

E-1099

Stator specifications	Stage					
	1	2	3	4	5	6
α, deg	21.0	17.5	17.5	17.5	17.5	17.5
t, in.	0.054	0.066	0.066	0.066	0.066	0.066
s, in.	0.173	0.254	0.254	0.254	0.254	0.254
Number of passages	1	4	7	11	21	44
Percent arc of admission	0.69	4.04	7.07	11.11	21.21	44.44
Throat area, sq in.	0.0135	0.0660	0.1156	0.1815	0.3467	0.7260

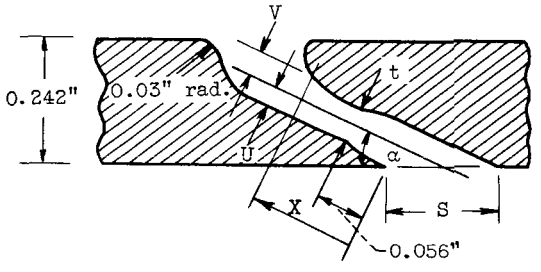

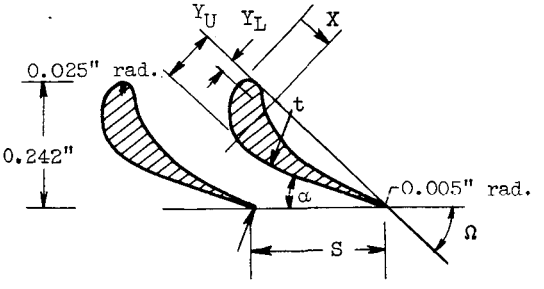

First-stage stator

X	U	V	X	U	V
0	0.0308	0.0308	0.100	0.0256	0.0302
.005	.0307	.0307	.120	.0242	.0342
.010	.0306	.0306	.140	.0226	.0414
.015	.0304	.0304	.160	.0208	.0542
.020	.0302	.0302	.180	.0184	.0764
.025	.0298	.0298	.190	------	.0946
.030	.0295	.0295	.200	.0154	.1262
.035	.0290	.0290	.220	.0116	------
.040	.0286	.0286	.240	.0064	------
.045	.0281	.0281	.260	-.0014	------
.050	.0277	.0277	.280	-.0120	------
.055	.0273	.0273	.300	-.0266	------
.056	.0272	.0272	.320	-.0460	------
.060	.0272	.0272	.340	-.0700	------
.080	.0266	.0282	.3434	-.0748	------

Second- to sixth-stage stator; Ω, 35°58'

X	Y_L	Y_U
0	0.0250	0.0250
.040	.0050	.0876
.080	.0280	.1030
.120	.0410	.1032
.160	.0464	.0945
.200	.0461	.0819
.240	.0416	.0685
.280	.0346	.0552
.320	.0261	.0419
.360	.0161	.0284
.400	.0042	.0150
.4184	.0050	.0050

(a) Stator.

Figure 2. - Mean-radius blading, dimensions, and coordinates for six-stage reentry turbine.

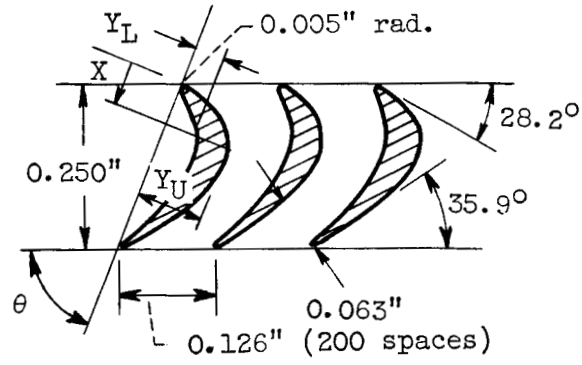

Rotor; θ, 70°55'

X	Y_L	Y_U	X	Y_L	Y_U	X	Y_L	Y_U
0	0.0050	0.0050	0.100	0.0578	0.1018	0.200	0.0347	0.0524
.020	.0185	.0648	.120	.0576	.0973	.220	.0243	.0385
.040	.0375	.0862	.140	.0551	.0895	.240	.0118	.0245
.060	.0490	.0975	.160	.0503	.0790	.260	0	.0106
.080	.0551	.1022	.180	.0435	.0664	.2645	.0050	.0050

(b) Rotor.

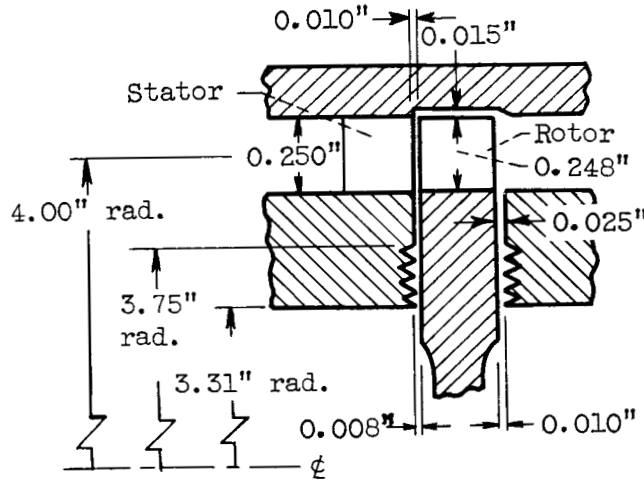

(c) Stator-rotor clearances.

Figure 2. - Concluded. Mean-radius blading, dimensions, and coordinates for six-stage reentry turbine.

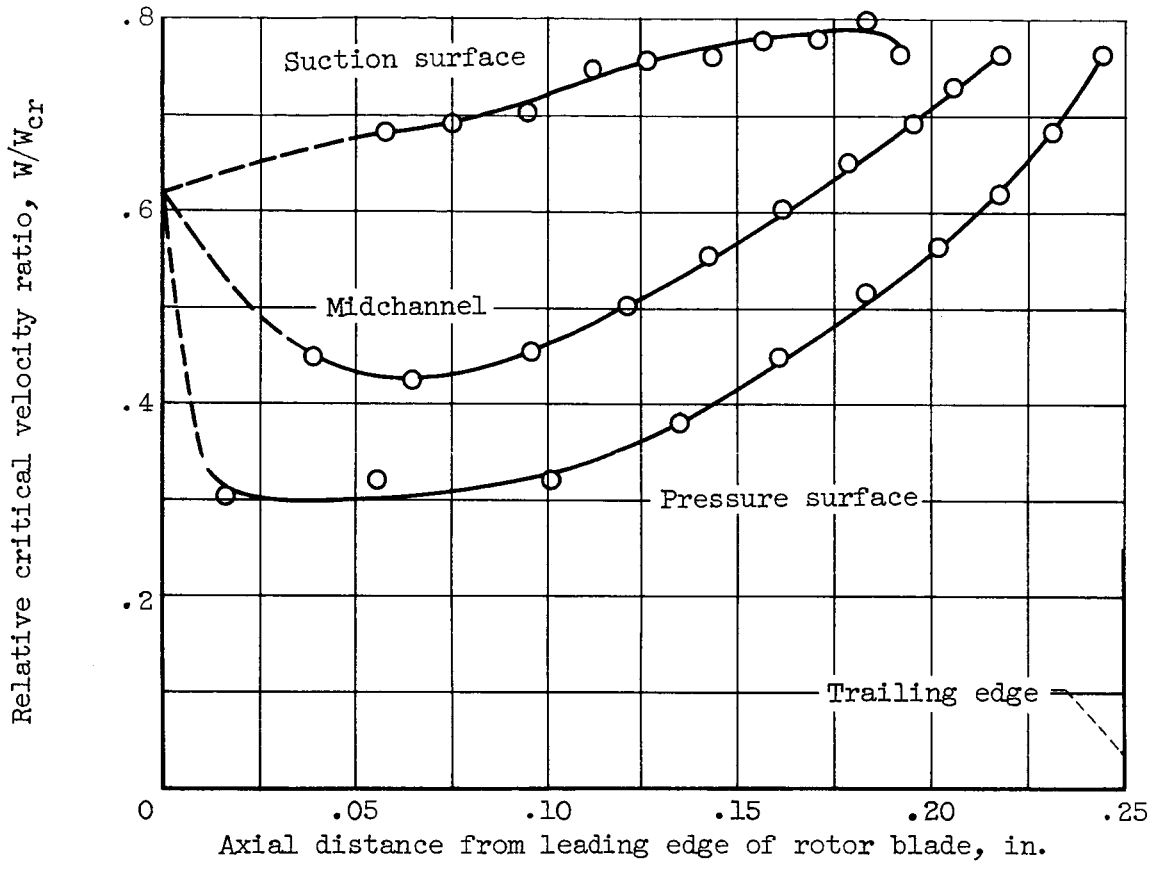

Figure 3. - Sixth-stage-rotor mean-radius channel velocity distribution.

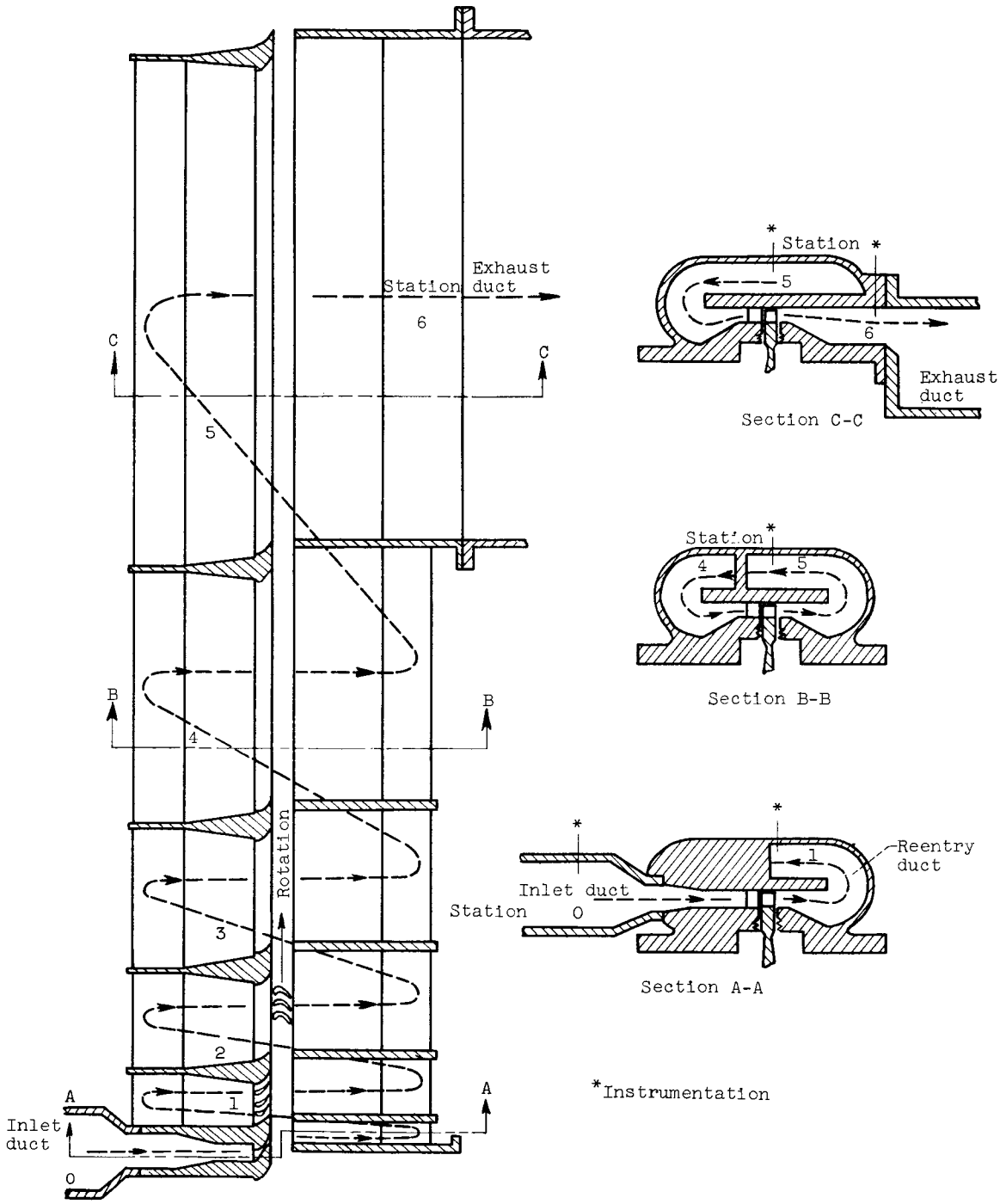

Figure 4. - Turbine reentry ducting and casing configuration.

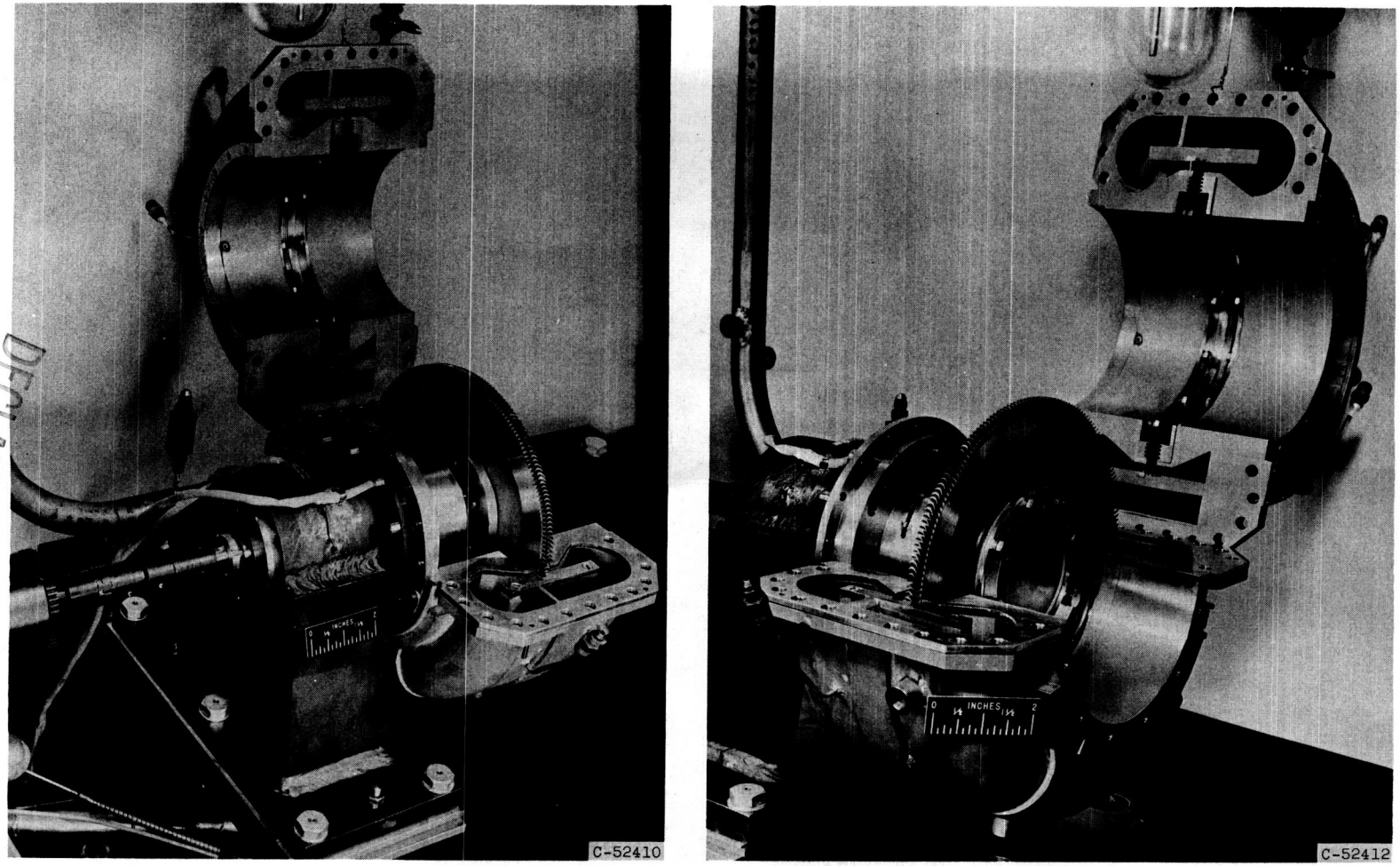

Figure 5. - Six-stage reentry turbine.

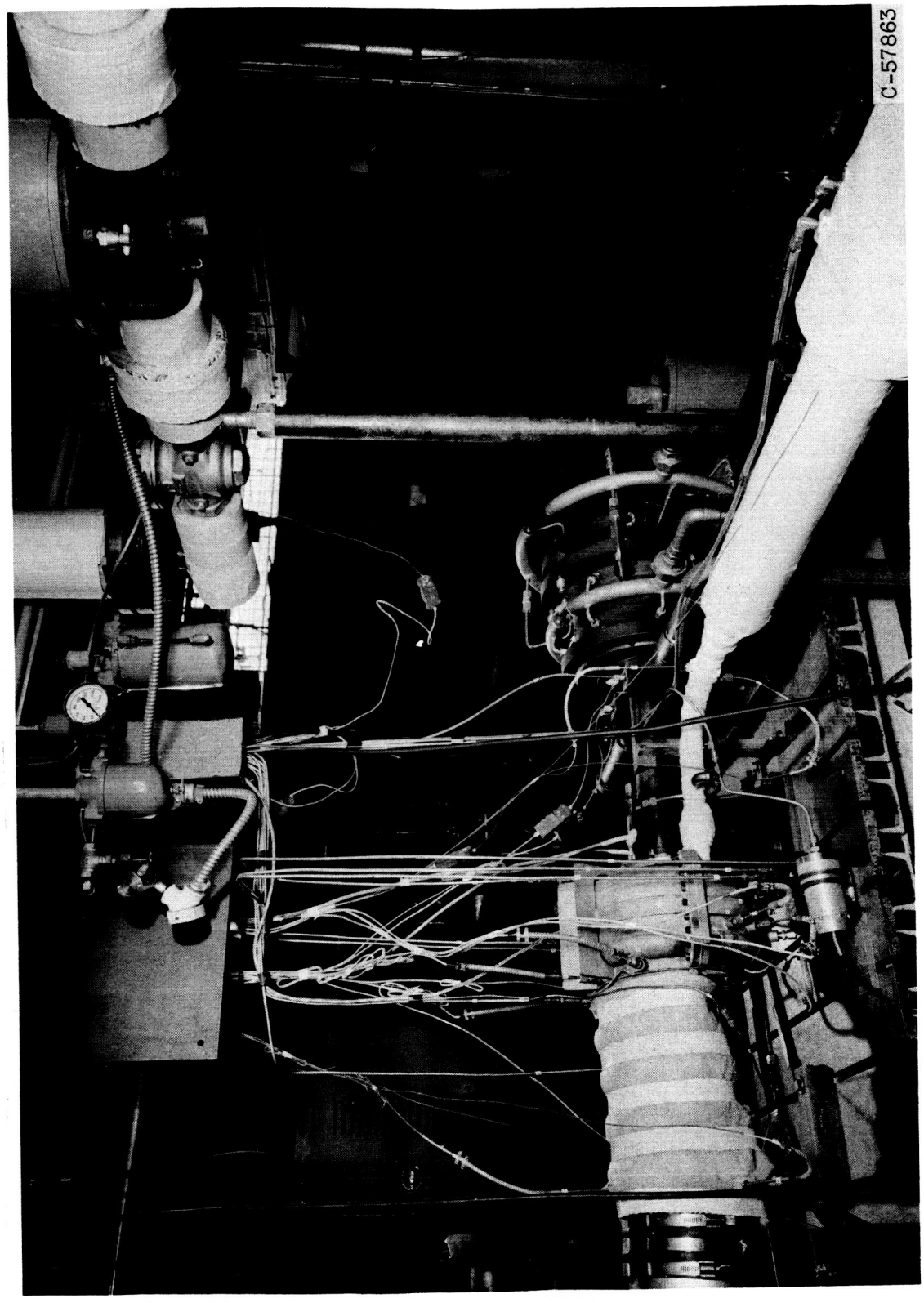

Figure 6. - Six-stage reentry turbine and facility.

E-1099

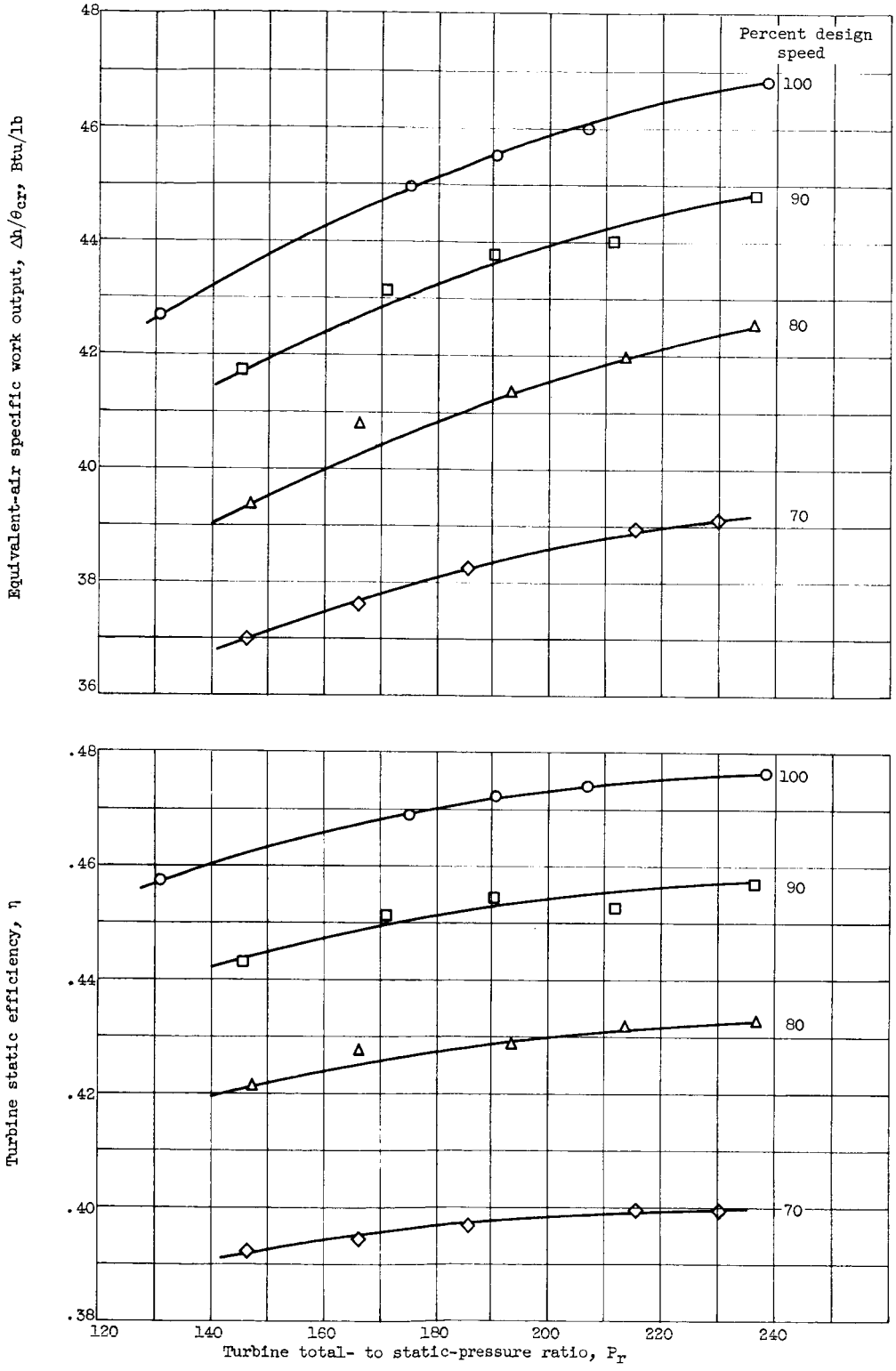

Figure 7. - Variation of equivalent-air specific work output and turbine static efficiency with pressure ratio for six-stage reentry turbine.

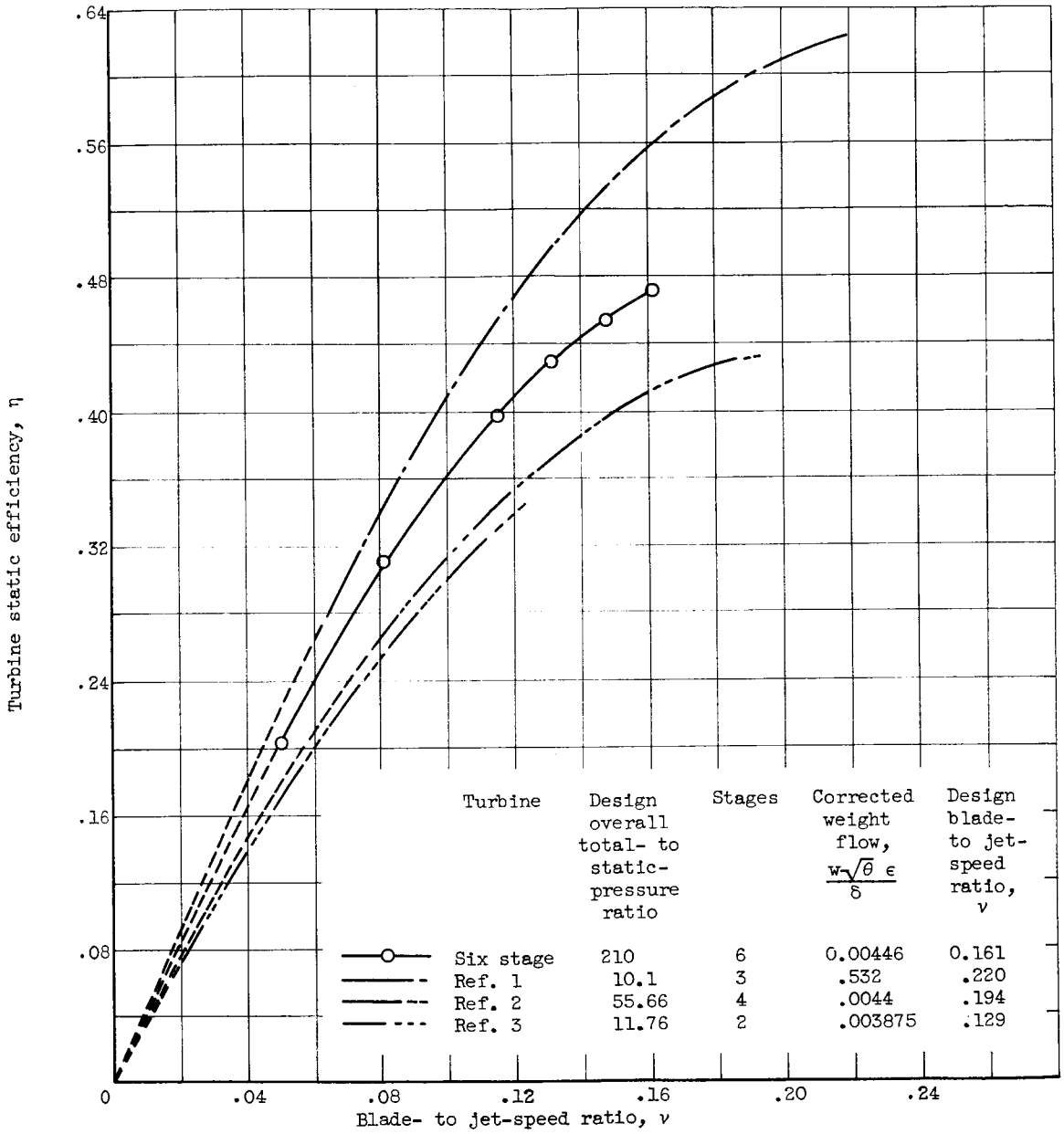

Figure 8. - Variation of turbine static efficiency with blade- to jet-speed ratio at design pressure ratio.

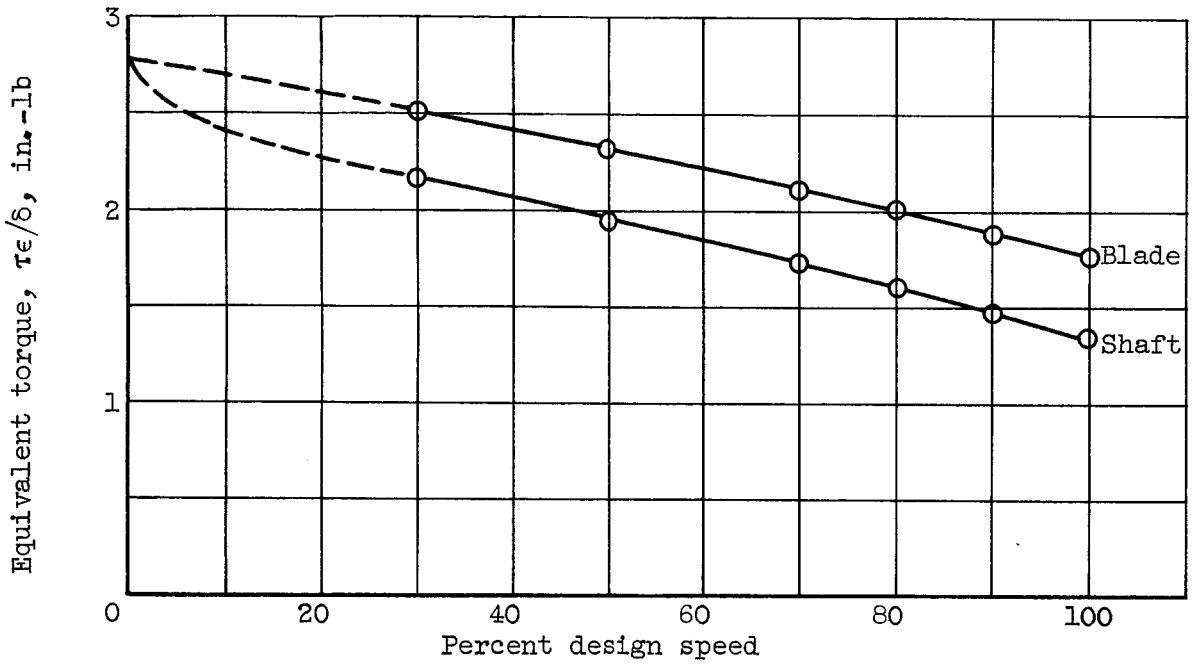

Figure 9. - Variation of equivalent torque with speed at design pressure ratio for six-stage reentry turbine.

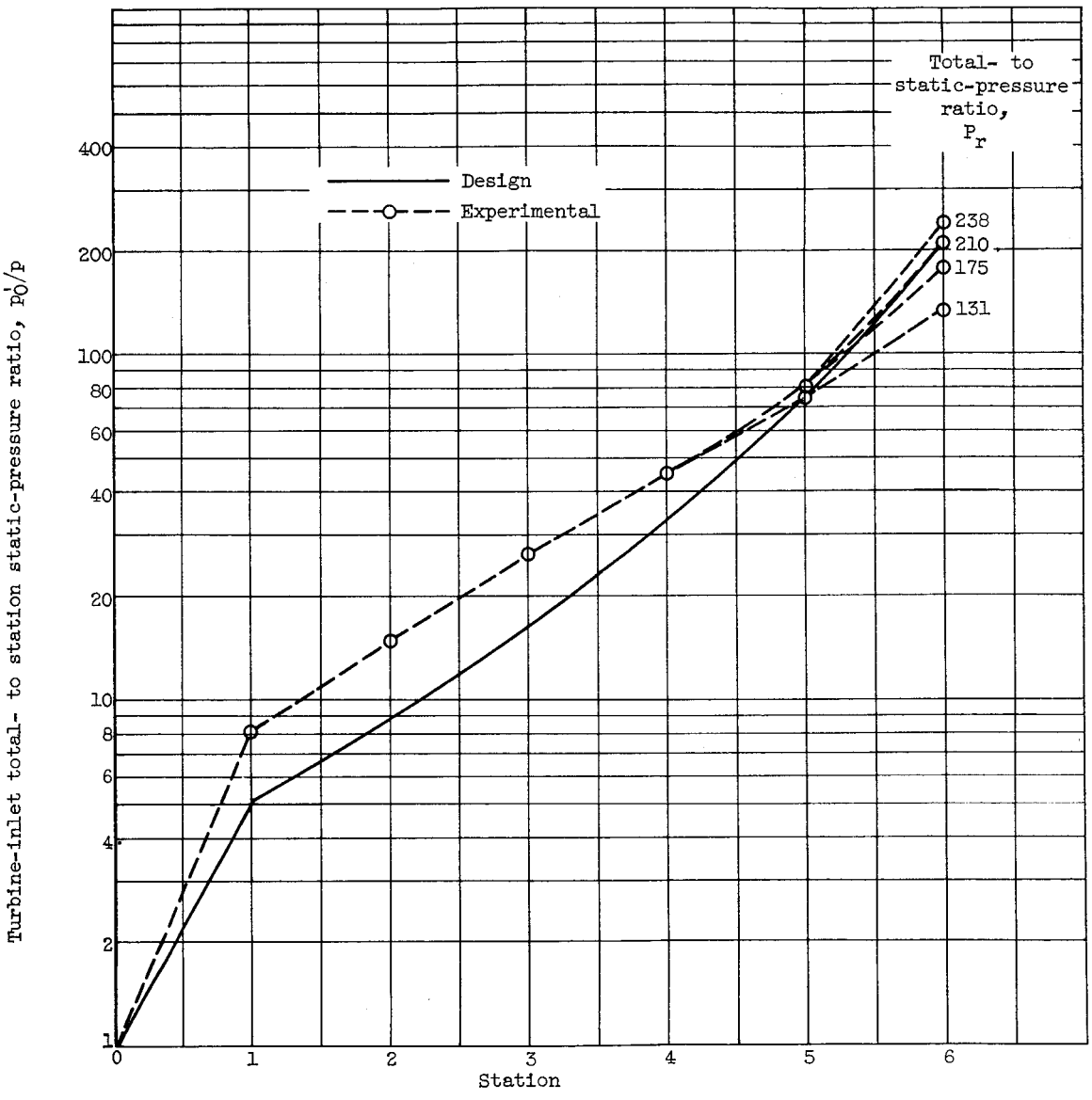

Figure 10. - Interstage static-pressure distribution.